Applied Surface Science 257 (2011) 9152–9157

Contents lists available at ScienceDirect

Applied Surface Science

journal homepage: www.elsevier.com/locate/apsusc

Tunable wettability of carbon nanotube/poly (ε-caprolactone) hybrid films

Chih-Feng Wang[a,*], Chih-Siang Liao[a], Shiao-Wei Kuo[b], Han-Ching Lin[c]

[a] Department of Materials Science and Engineering, I-Shou University, Kaohsiung, 840, Taiwan
[b] Department of Materials and Optoelectronic Science, Center for Nanoscience and Nanotechnology, National Sun Yat-Sen University, Kaohsiung, 804, Taiwan
[c] National Nano Device Laboratories, 300, Hsinchu, Taiwan

ARTICLE INFO

Article history:
Received 15 February 2011
Received in revised form 30 May 2011
Accepted 30 May 2011
Available online 6 June 2011

Keywords:
Carbon nanotubes
Superhydrophobic
Reversible
Mobility

ABSTRACT

We have realized a stable superhydrophobic surface, a thermally tunable superhydrophobic surface, and a thermally tunable hydrophobic surface by combining the crystalline/amorphous phase transition of the poly(ε-caprolactone) (PCL) with the optimized surface roughness of the carbon nanotube/PCL hybrid films. The water droplet mobilities and wettabilities were reversibly thermally switched on the tunable superhydrophobic and the hydrophobic surfaces, respectively. These responsive surfaces have potential applications in microfluidic devices and microreactors and for liquid transportation.

1. Introduction

Liquid repellency is an important property influencing a material's applications. The wettability of a solid surface can be controlled by varying its topographical microstructures and/or its surface chemistry [1–7]. Many effective methods have been developed to prepare a range of superhydrophobic and hydrophobic films exhibiting controllable wettability. Ran et al. reported that the wettability of an ordered nanoporous alumina surface could be changed from hydrophilic to hydrophobic by increasing the hole diameter or depth [8]. Gao and co-workers designed three types of superhydrophobic porous-nanostructure models exhibiting controllable adhesive forces to water, ranging from very high to extremely low, by tuning microstructures of TiO_2 films [9]. Jiang and co-workers. prepared a unique water-repellent material covered with ribbed, conical copper hydroxide nanoneedles [10]; the as-prepared superhydrophobic surface exhibited robust superhydrophobicity with little contact-angle hysteresis even under varying hydrostatic pressure.

The wettability of a rugged surface can also be altered by changing its surface chemistry. Many surfaces exhibiting stimuli-responsive wettability have been developed, e.g., photoresponsive surfaces allowing the light-driven motion of liquids, [11] surface that switch reversibly under applied electric potentials, [12,13] stimuli-responsive surfaces controlled by pH or ultraviolet (UV) irradiations, [14–17] and others [18,19]. Changing the temperature is a widely used environmental stimulus for responsive materials. To date, most thermo-responsive surfaces have been prepared using polymers having a lower critical solution temperature (LCST) [20–22]. Jiang and co-workers reported that when the temperature is above the LCST, the compact, collapsed conformation of poly(*N*-isopropylacrylamide) (PNIPAAm) chains induced by intramolecular hydrogen bonding between the C=O and N–H groups in the main chains, leads to high contact angles for water [22]. When the temperature is below the LCST, the predominant intermolecular hydrogen bonding between the PNIPAAm main chains and water molecules leads to lower water contact angles.

Poly(ε-caprolactone) (PCL) has recently been classified as a new thermo-responsive material [23]. PCL chains possess hydrophilic end groups (COOH, OH), hydrophobic groups [$(CH_2)_5$], and amphiphilic ester groups. At temperatures below the phase transition point, water droplets come into contact mostly with the hydrophobic groups, resulting in higher water contact angles. When the phase transition temperature is reached, the polymer chains are much more mobile and their reorientation can be induced by contact with water. This phenomenon results in the presence of hydrophilic and amphiphilic groups at the water–PCL interface, thereby decreasing the water contact angle. In this present study, we developed three types of carbon nanotube (CNT)/PCL hybrid films: a stable superhydrophobic surface, a tunable superhydrophobic surface, and a tunable hydrophobic surface. We prepared these multifunctional CNT/PCL hybrid films under ambient conditions using readily available raw

* Corresponding author. Tel.: +886 7 6577711 3129; fax: +886 7 6578444.
E-mail address: cfwang@isu.edu.tw (C.-F. Wang).

0169-4332/$ – see front matter © 2011 Elsevier B.V. All rights reserved.
doi:10.1016/j.apsusc.2011.05.121

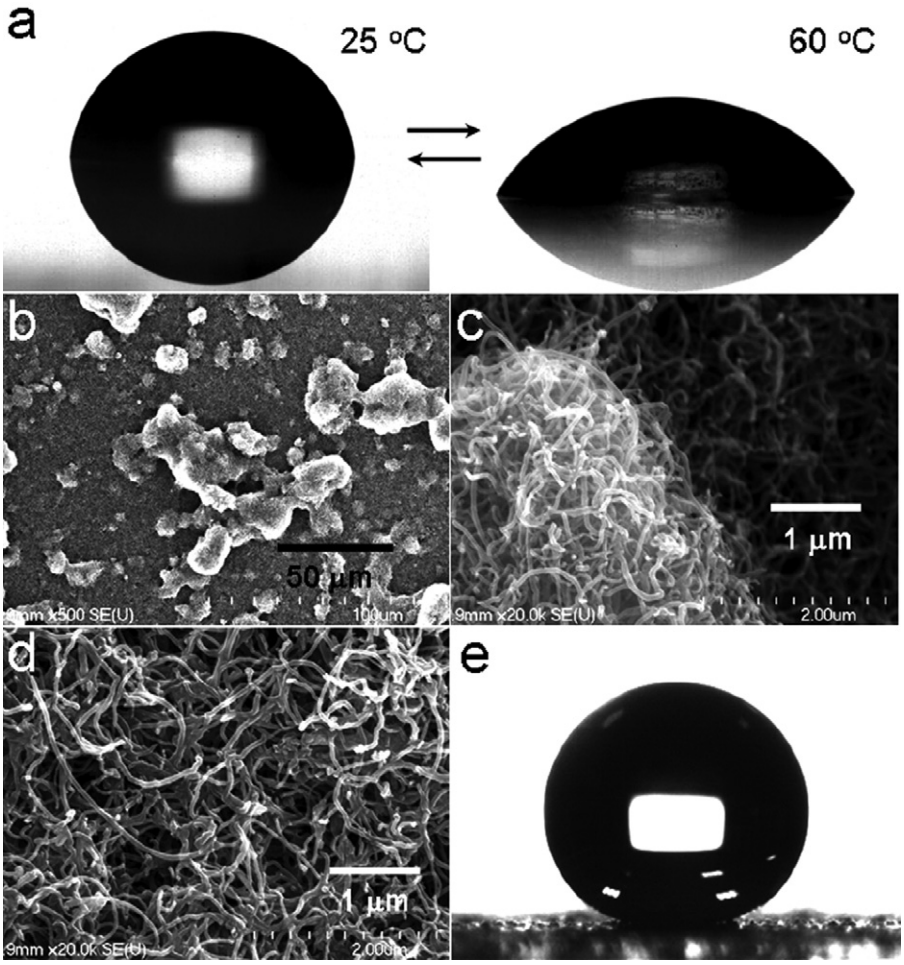

Fig. 1. (a) Water droplet profiles at temperatures at 25 and 60 °C: water contact angles: 87 ± 2° and 59 ± 2°, respectively. (smooth PCL films) (b) Large-area SEM image of the as-prepared rough CNT substrate: scale bar: 50 μm. (c) Enlarged view of a micro-island in (b): scale bar: 1 μm. (d) SEM image of the lower surface of the rough CNT substrate: scale bar: 1 μm. (e) Profile of a water drop on the rough CNT substrate.

materials and laboratory equipment. Here, we report a systematic study of the influences of the morphology and surface chemistry on the wetting state of these CNT/PCL hybrid surfaces.

2. Experimental

2.1. Materials

PCL was prepared through ring opening polymerization of ε-caprolactone according to the previous study [24]. The polymerization was initiated with benzyl alcohol by using a catalytic amount of stannous octoate [$Sn(oct)_2$] and then performed in the melt at 120 °C (20 h). The polymer was then dissolved in tetrahydrofuran (THF) and precipitated from cold methanol. The resulting polymer was filtered and dried overnight at 40 °C under vacuum to obtain a white powder. The number-average molecule weight (M_n) and polydispersity index (PDI) of the synthesized PCL were 14800 g/mol and 1.22, respectively. Sylgard 184, a poly(dimethylsiloxane) (PDMS), was supplied by Dow Corning. Multiwalled carbon nanotubes (average diameter: 20–40 nm; length: 5–15 μm) were purchased from Conyuan Biochemical Technology. Water that had been purified through reverse osmosis was further purified using a Millipore Milli-Q system.

2.2. Sample fabrication

The PCL films were deposited on flat glass slides and the rough CNT surfaces. The rough CNT substrates were prepared on glass slides using a two-step process. First, PDMS (Sylgard 184A, 0.1 g) was mixed with curing agent (Sylgard 184B, 0.01 g) in toluene (10 mL) and then the solution was spin-coated (1500 rpm, 45 s) onto a glass slide using a photoresist spinner. Second, a CNT/EtOH suspension (1 mg/mL, sonicated for 30 min prior to use) was sprayed onto the PDMS surface, which was positioned on a heating plate held at 90 °C and then cured in an oven at 150 °C for 1 h. The rough CNT surfaces were then modified with PCL films. The PCL solutions (in THF) of various concentrations (Table 1), were spin-coated (1500 rpm, 45 s) onto the rough surfaces. The samples were then stored in a chamber for 12 h before heating under vacuum at 120 °C for 4 h to remove any residual solvent.

Table 1
Experimental conditions for the production of the CNT/PCL hybrid films.

Sample	Concentration of PCL solution (g/mL)
1	0
2	0.03
3	0.10
4	0.15
5	0.20

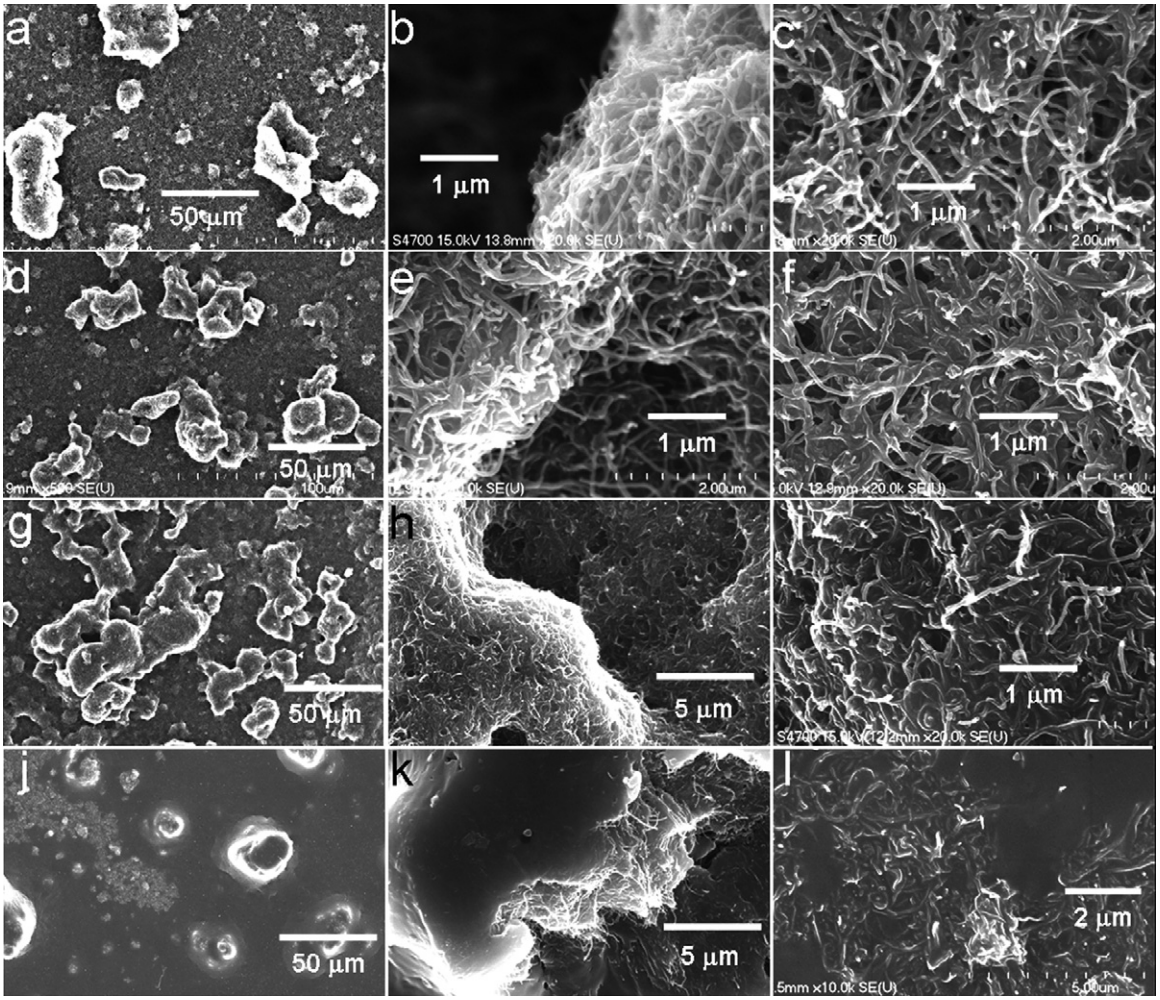

Fig. 2. Low and high magnification SEM images of the CNT/PCL hybrid films: (a–c) sample 2; (d–f) sample3; (g–i) sample4; (j–l) sample5. Scale bars: (a, d, g, j) 50 μm; (b, c, e, f, i) 1 μm; (h, k) 5 μm; (l) 2 μm.

2.3. Characterization

The microstructures of the CNT/PCL hybrid films were characterized using a HITACHI-S-4700 scanning electron microscope (acceleration voltage: 5 kV); each specimen was coated with a thin layer of Pt/Pd prior to observations. Static contact angles and sliding angles were measured for 5 μL drops using a FDSA MagicDroplet-100 contact angle goniometer. Each of the reported contact angles represents the average of six measurements. The water evaporation experiments were carried out at room temperature (24–27 °C) and relative humidity (45–60%) in an enclosure to shield from drafts. X-ray photoelectron spectroscopy (XPS) were performed using a VG Microlab 310F spectrometer with an Al Kα X-ray source (1486.6 eV).

3. Results and discussion

After spin-coating PCL on a glass slide and then heating under vacuum at 120 °C for 4 h; we obtained a smooth surface. This PCL thin film exhibited a water contact angle that switched between $87 \pm 2°$ at 25 °C and $59 \pm 2°$ at 60 °C (Fig. 1a). Wettability switching can be enhanced through a suitable combination of responsive materials and rough surfaces. In this study, we constructed rough substrates from CNT binary structures produced by spraying CNT suspensions onto PDMS-modified glass slides [25]. This rough substrate (sample 1) possessed both micro- and nano-scale binary structures. Many micro-islands (5–20 μm) were present on this surface in a random distribution (Fig. 1b); in the micro-islands, hierarchical structures existed in the form of branch-like nanostructures having diameters of 20–40 nm (Fig. 1c). Nanostructures were also present on the lower surface of the rough substrate (Fig. 1d). The as-prepared rough CNT substrate exhibited superhydrophobicity, with a high water contact angle ($165 \pm 1°$, Fig. 1e) and a low sliding angle (<3°). We modified this rough CNT substrate with PCL films under various experimental conditions (Table 1).

Scanning electron microscopy (SEM) images of sample 2 revealed (Fig. 2a–c) that PCL was deposited mainly on the lower surface of the rough substrate and did not result in a significant morphological change relative to sample 1. In sample 3 (Fig. 2d), PCL was present on both the micro-islands (Fig. 2e) and lower surfaces (Fig. 2f); the branch-like CNT nanostructures were connected together by the PCL films. Increasing the amount of PCL in the composite film (sample 4) caused a portion of the CNT nanostructures to be embedded in the PCL films (Fig. 2g–i) but micro- and nano-scale binary structures remained. A further increase in the amount of PCL (sample 5) resulted in the rough CNT substrate being entirely covered by the PCL films (Fig. 2j). Magnified SEM images of the cracks of the micro-islands (Fig. 2k) and lower surfaces (Fig. 2l) revealed that the CNT nanostructures in sample 5 were fully embedded within the PCL films; therefore, this sample possessed rough structures only on the micro-scale.

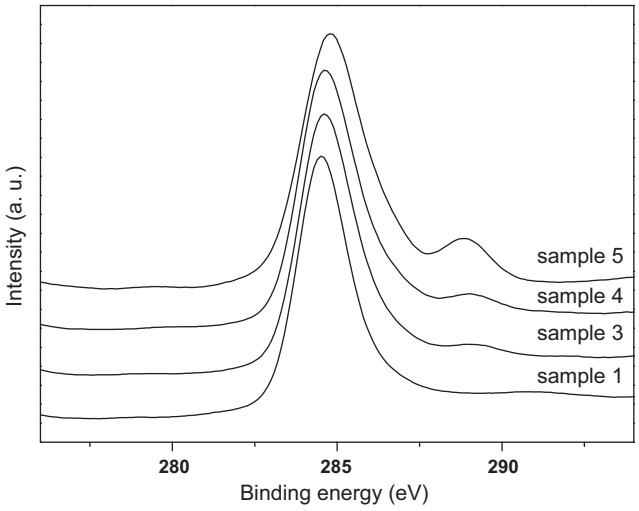

Fig. 3. XPS C(1s) spectra of the CNT/PCL hybrid films.

We used XPS to identify the functional groups attached to the surfaces of the CNT/PCL hybrid films. Fig. 3 displays the XPS C 1s spectra of the rough CNT substrates before and after treatment with PCL. The peak at 289.1 eV is the signal of the O–C=O groups of the PCL main chain [26]. This peak was present in the spectra of samples 3–5. The XPS analyses were consistent with the SEM images: PCL was generated on samples 3–5.

Fig. 4 displays photographs of water droplets on samples 3–5 at both 25 and 60 °C. For sample 3, the variation in temperature did not significantly affect the wettability; this CNT/PCL hybrid films provided high water contact angles ($163 \pm 2^\circ$) and small sliding angles (<3°) at both temperatures (Fig. 4a). This observation can be explained using Eq. (1), which Cassie and Baxter derived to describe the contact angle for a liquid droplet at an air–solid composite surface [27].

$$\cos\theta_c = f_1(\cos\theta + 1) - 1 \quad (1)$$

where θ is the intrinsic contact angle on a smooth surface, θ_c is that on a rough air–solid composite surface made of the same material, and f_1 and $(1-f_1)$ are the area fractions of the solid–liquid and air–liquid interfaces relative to the projected surface area, respectively. Sample 3 featured a micro- and nano-scale binary structure the high surface roughness of which led to the formation of composite interfaces in which air was trapped within the grooves beneath the liquid; this phenomenon significantly minimized the contact area between the CNT/PCL surface and the liquid. The wetting states on sample 3 at both 25 and 60 °C were most likely Cassie states. The apparent contact angle of a rough surface is always high in the Cassie state because of the existence of air pockets, regardless of the wettability of the primary surface (in some cases, the superhydrophobic surfaces can be prepared from hydrophilic materials) [28,29]. We classify sample 3 as a stable superhydrophobic surface; the water contact angle of the films remained nearly unchanged upon varying the temperature, even around the phase transition temperature of PCL.

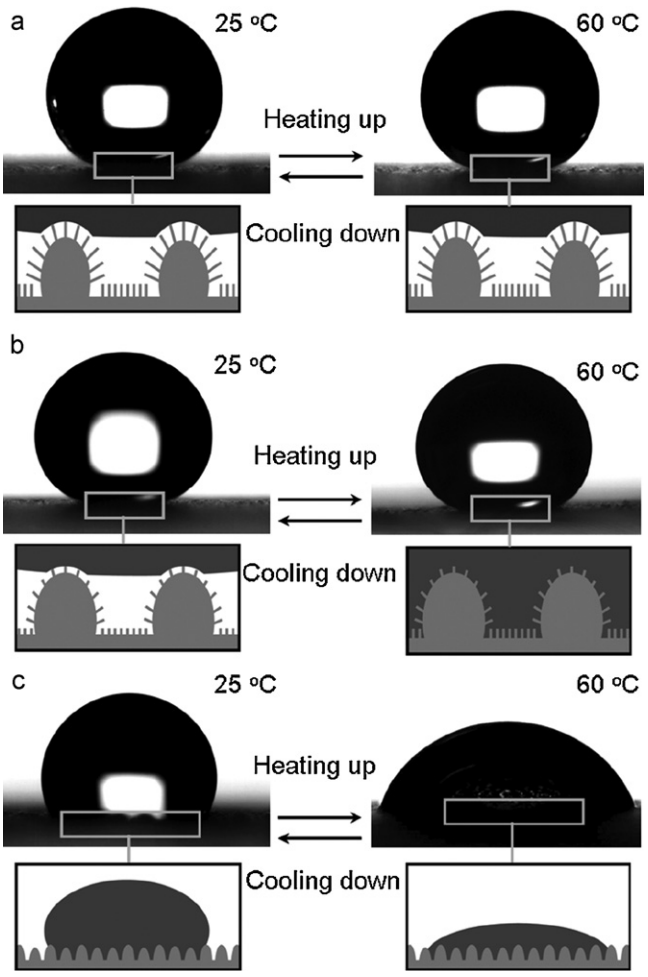

Fig. 4. Water droplets profiles and wettability states of the CNT/PCL hybrid films at 25 and 60 °C: (a) sample 3; (b) sample 4; (c) sample5.

In sample 4, the increased amount of PCL in the composite film reduced the nano-scale roughness and had a greater impact on the wettability (Fig. 4b). At 25 °C, this sample existed in a persistent superhydrophobic composite state (Cassie state); water droplets possessed near-spherical shapes (contact angle: $160 \pm 2^\circ$) and rolled off with ease (sliding angle: ca. 6°). The water contact angles on sample 4 remained in the superhydrophobic range ($151 \pm 3^\circ$) at 60 °C but a sudden switching of the droplet mobility—from rollable

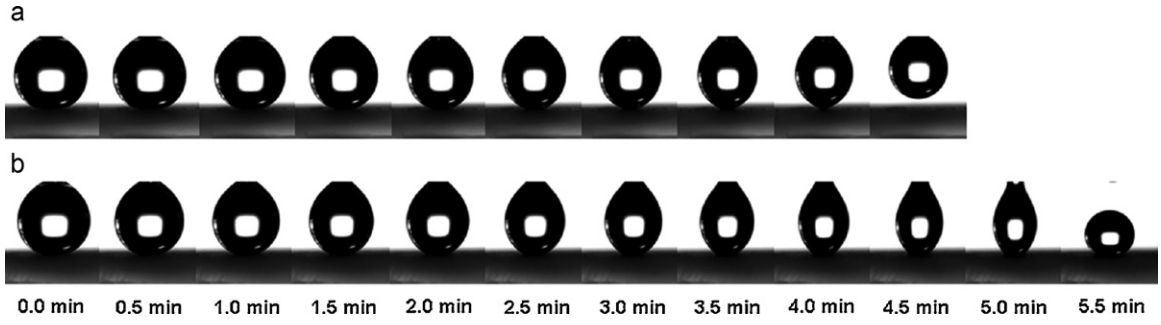

Fig. 5. Photographs of water droplets (initial volume of 5 μL) evaporating at 60 °C on (a) sample 3 and (b) sample 4.

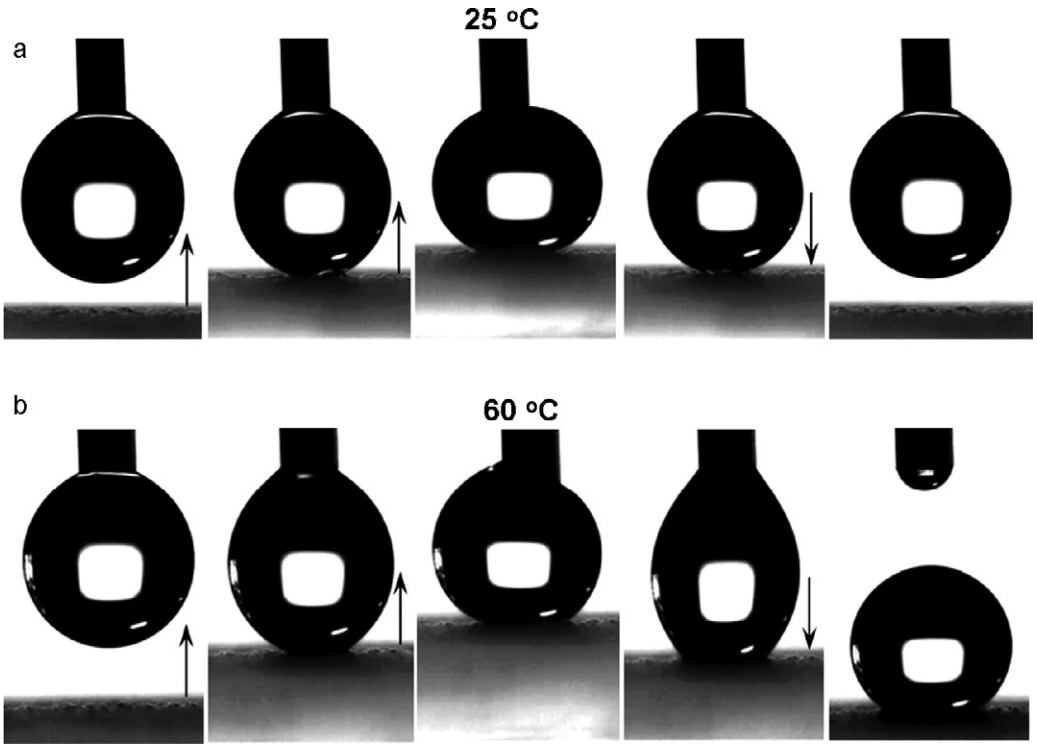

Fig. 6. Approach, contact, deformation, and departure processes of a 4 μL water droplet suspended on a syringe with respect to the CNT/PCL hybrid films of sample 4 at (a) 25 °C and (b) 60 °C. Arrows indicate the direction of the movement of the substrate.

to pinned (sliding angle: >90°)—occurred with the phase transition. Fig. 4b reveals a spherical water droplet in the superhydrophobic composite state of the sample at 25 °C and in the superhydrophobic wetted state at 60 °C. Thus, the water droplet mobility on sample 4 could be controlled by varying the temperature.

In sample 5, the presence of PCL on the composite surface greatly reduced the roughness and caused lower hydrophobicity. At 25 °C, water droplet on the sample 5 existed in the hydrophobic state, with the contact angle of ca. 114°. At the phase transition temperature (60 °C) the contact molds between the water droplets and the CNT/PCL hybrid films switched from a hydrophobic wetted state to a hydrophilic state (contact angle: 69 ± 3°). Thus, sample 5 possessed thermally tunable hydrophobicity (Fig. 4c).

The evaporation process provided important information on the determination of superhydrophobic states (i.e., a Cassie state or a Wenzel state) [30,31]. Fig. 5 displays a set of the captured images of water droplets undergoing evaporation on the two different substrates at 60 °C. On the sample 3, the contact area of the water droplet decreased continuously over time (Fig. 5a), but it maintained its spherical shape until it completely departed from the surface. Contact angle hysteresis is an important criterion for characterizing the hydrophobicity of a solid surface: it can be regarded as the force required to move a liquid droplet across a surface. When the contact angle hysteresis is small or negligible, only a very small force is required to move the droplet. The observation of the contact angle changing with time for sample 3 in Fig. 5a (because of evaporation, the angle became a receding angle) determines a superhydrophobic composite state (Cassie state) of comparable receding angle for the water drop [32]. In contrast, the water droplet was pinned on sample 4 at 60 °C, with the contact area decreasing slightly during the evaporation process; eventually, the water droplet withdrew from the needle and deposited on the surface (Fig. 5b). This behavior indicates that the surface of sample 4 at 60 °C (superhydrophobic wetted state) possessed a greater adhesion force toward water than did sample 3 at the same temperature.

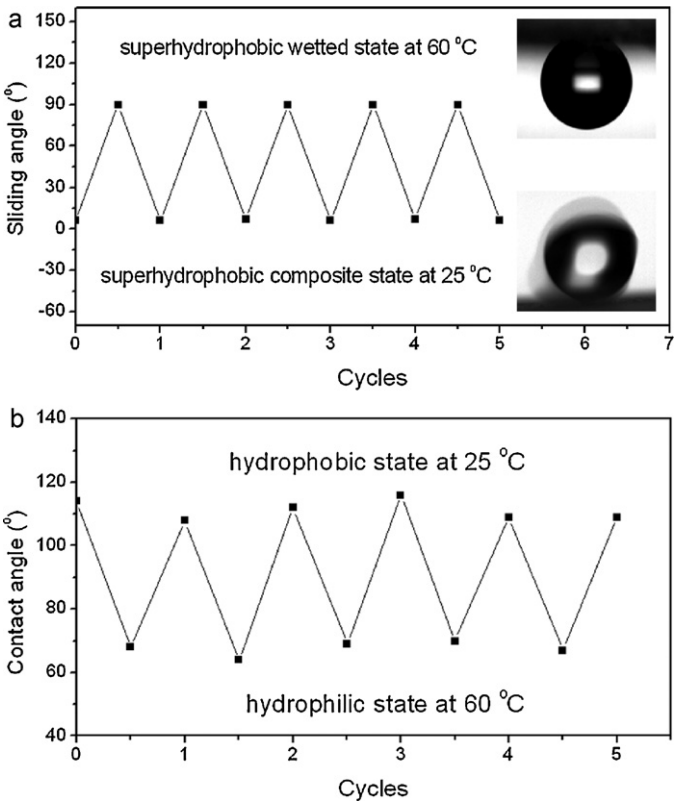

Fig. 7. Five cycles of temperature-dependent (between 25 and 60 °C) reversible switching of (a) the water droplet mobility (from rollable to pinned) on sample 4. (b) the wettability of sample 5.

We also used the method reported by Gao et al. [33] to test the adhesion of a water droplet on sample 4 at 25 and 60 °C. Fig. 6 displays the approach—contact, deformation, and departure of a 4 μL water droplet suspended on a syringe—for sample 4 at various temperatures. The water droplet readily and completely departed from the surface of sample 4 at 25 °C (superhydrophobic composite state), even though severe deformation occurred in this case (Fig. 6a). In contrast, the water droplet remained steady on the surface of sample 4 at 60 °C (superhydrophobic wetted state: Fig. 6b), because the microstructure of the superhydrophobic wetted state, filled with water, greatly enhanced the adhesion force toward water droplets [34].

For samples 4 and 5, we repeatedly cycled the temperature between 25 and 60 °C and recorded the water droplets mobility and wettability. Fig. 7a reveals the excellent reversible switching of the water droplet's mobility, between rollable and pinned for sample 4. Similarly, the sample 5 exhibited highly reversible switching of its wettability between hydrophobic and hydrophilic (Fig. 7b).

4. Conclusions

We have developed a simple and inexpensive method for fabricating multifunctional CNT/PCL hybrid films exhibiting different types of surface chemistry and surface roughness and thereby, enhanced stimuli-responsive wettability. We prepared three hybrid films exhibiting stable superhydrophobicity (sample 3), thermally tunable superhydrophobicity (sample 4), and thermally tunable hydrophobicity (sample 5), respectively. These samples displayed highly reversible switching of the mobility of water droplets (between rollable and pinned) and of their wettability (between hydrophobic and hydrophilic). The wetting states for these samples were dependent on the trade-off between surface morphology (micro- and nano-scale roughness) and surface chemistry (thermoresponsive hydrophobicity and hydrophilicity).

Acknowledgements

This study was supported financially by the National Science Council, Taiwan, Republic of China (contract NSC 99-2221-E-214 -005) and I-Shou University (contract ISU 98-S-03). We thank the National Nano Device Laboratories for technical support.

References

[1] Y. Guo, Q. Wang, Appl. Surf. Sci. 257 (2010) 33.
[2] J. Wang, X. Chen, Y. Kang, G. Yang, L. Yu, P. Zhang, Appl. Surf. Sci. 257 (2010) 1473.
[3] K.S. Liu, X. Yao, L. Jiang, Chem. Soc. Rev. 39 (2010) 3240.
[4] C.R. Crick, I.P. Parkin, Chem. Eur. J. 16 (2010) 3568.
[5] B.W. Xin, J.C. Hao, Chem. Soc. Rev. 39 (2010) 769.
[6] M.J. Liu, Y.M. Zheng, J. Zhai, L. Jiang, Acc. Chem. Res. 43 (2010) 368.
[7] D. Quéré, Annu. Rev. Mater. Res. 38 (2008) 71.
[8] C. Ran, G. Ding, W. Liu, Y. Deng, W. Hou, Langmuir 24 (2008) 9952.
[9] Y. Lai, X. Gao, H. Zhuang, J. Huang, C. Lin, L. Jiang, Adv. Mater. 21 (2009) 3799.
[10] X. Yao, Q. Chen, L. Xu, Q. Li, Y. Song, X. Gao, D. Quéré, L. Jiang, Adv. Funct. Mater. 20 (2010) 656.
[11] K. Ichimura, S.K. Oh, M. Nakagawa, Science 298 (2002) 1624.
[12] J. Lahann, S. Mitragotri, T. Tran, H. Kaido, J. Sundaram, I.S. Choi, S. Hoffer, G.A. Somorjai, R. Langer, Science 299 (2003) 371.
[13] Z. Han, B. Tay, C. Tan, M. Shakerzadehand, K. Ostrikov, ACS Nano 3 (2009) 3031.
[14] X. Yu, Z.Q. Wang, Y.G. Jiang, F. Shi, X. Zhang, Adv. Mater. 17 (2005) 1289.
[15] X. Zhu, Z. Zhang, X. Men, J. Yang, X. Xu, Appl. Surf. Sci. 256 (2010) 7619.
[16] A. Hozumi, S. Kojima, S. Nagano, T. Seki, N. Shirahata, T. Kameyama, Langmuir 23 (2007) 3265.
[17] Y.G. Jiang, P.B. Wan, M. Smet, Z.Q. Wang, X. Zhang, Adv. Mater. 20 (2008) 1972.
[18] G.Y. Qing, X. Wang, L. Jiang, H. Fuchs, T.L. Sun, Soft Matter 5 (2009) 2759.
[19] L. Ionov, N. Houbenov, A. Sidorenko, M. Stamm, I. Luzinov, S. Minko, Langmuir 20 (2004) 9916.
[20] J. Gao, Y. Liu, H. Xu, Z. Wang, X. Zhang, Langmuir 26 (2010) 9673.
[21] N. Wang, Y. Zhao, L. Jiang, Macromol. Rapid Commun. 29 (2008) 485.
[22] T. Sun, G. Wang, L. Feng, B. Liu, Y. Ma, L. Jiang, D. Zhu, Angew. Chem. Int. Ed. 43 (2004) 357.
[23] S. Hu, X. Cao, Y. Song, C. Li, P. Xie, L. Jiang, Chem. Commun. (2008) 2025.
[24] S.W. Kuo, C.F. Huang, C.H. Lu, H.M. Lin, K.U. Jeong, F.C. Chang, Macromol. Chem. Phys. 207 (2006) 2006.
[25] C.F. Wang, W.Y. Chen, H.Z. Cheng, S.L. Fu, J. Phys. Chem. C 114 (2010) 15607.
[26] P. Viville, R. Lazzaroni, Langmuir 19 (2003) 9425.
[27] A.B.D. Cassie, S. Baxter, Trans. Faraday Soc. 40 (1944) 546.
[28] L. Cao, H.H. Hu, D. Gao, Langmuir 23 (2007) 4310.
[29] M. Zhu, W. Zuo, H. Yu, W. Yang, Y. Chen, J. Mater. Sci. 41 (2006) 3793.
[30] G. McHale, S. Aqui, N.J. Shirtcliffe, M.I. Newton, H.Y. Erbil, Langmuir 21 (2005) 11053.
[31] H.Y. Erbil, G. McHale, M.I. Newton, Langmuir 18 (2002) 2636.
[32] M. Callies, D. Quéré, Soft Matter 1 (2005) 55.
[33] X.F. Gao, X. Yao, L. Jiang, Langmuir 23 (2007) 4886.
[34] C. Li, R. Guo, X. Jiang, S. Hu, L. Li, X. Cao, H. Yang, Y. Song, Y. Ma, L. Jiang, Adv. Mater. 21 (2009) 4254.